Geosynthetics, J. Kuwano & J. Koseki (eds)

Estimate of thermal stress of geomembrane using a thermal infrared imaging device

Nakayama, H., Shimaoka, T. & Komiya, T.
Institute of Environmental Systems, Graduate School of Engineering, Kyushu University, Japan

Sannou, T
Fukuoka City, Japan

Keywords: geomembrane liner sheet, thermal stress, strain, thermal infrared image, FEM

ABSTRACT: In this study a new method to estimate thermal stress on geomembrane liner sheets caused by temperature changes was investigated. A thermographic device was used to obtain spatial distribution of the sheet temperatures then the data was input into the calculation of finite elements to estimate thermal stress. Results indicated that stress on the sheets varied depending on the direction of the light source. For example, the temperature gradient of the sheet on a concave corner of a landfill site is comparatively gentle as the sheet area surrounding the concave corner is warmed by both direct and reflected insolation. Conversely, sheets on a convex corner show a greater temperature difference as the insolation cannot reach areas of the sheet on the shady side. Finally, a simple simulation of a square-shaped landfill site was carried out to understand the transition of thermal stress changes as the sun moves during the day.

1 INTRODUCTION

Geomembrane landfill liner sheets expand and contract as the temperature changes. This occasionally causes extensive stress to the geomembranes and anchor trench if the sheets are installed without sufficient slack.

Under the experimental conditions where the upper and lower ends of a geomembrane sheet were securely fixed, the thermal stress initiated by a temperature change from 80 °C to –25 °C was 7.0 MPa in a high density polyethylene (HDPE) sheet and 0.12 MPa in a Ethylene Propylene Diene Monomer (EPDM) sheet[1].

Until now strain gauges have been used to measure the thermal stress on the geomembrane. The strain of geomembrane sheet installed in a sea-based landfill site was measured by strain gauges, and it was estimated about 3~15%[2]. However, the stress is at different places in a landfill site. It is difficult to understand spatial distribution of the stress and is also difficult to cover the entire liner sheet at a landfill site with strain gauges.

In this study a new method based on thermal infrared remote sensing was used to estimate the thermal stress on the geomembrane liner sheets caused by the temperature changes. To estimate thermal stress, a thermo graphic device was used to obtain spatial distribution of sheet temperatures then the data was input into the finite element method (FEM) calculation.

Finally, a simple simulation based on a square-shaped landfill site was carried out to understand the transition of thermal stress changes during daytime.

2 ESTIMATE OF THERMAL STRESS

2.1 *Experiments*

Experimental equipment using a geomembrane sheet was constructed to simulate three different configurations of a liner at a landfill site. Figures 1, 2 and 3 show the constructions for experiments on a

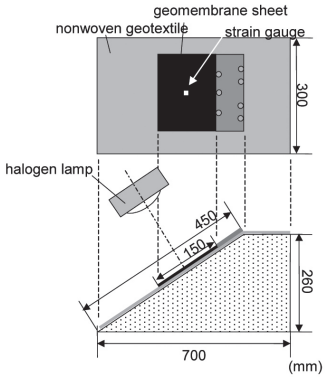

Figure 1. Experimental equipment for measuring thermal strain of a geomembrane on a simple slope.

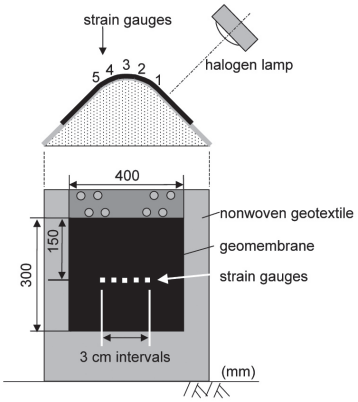

Figure 2. Experimental equipment for measuring thermal strain of a geomembrane on a convex corner.

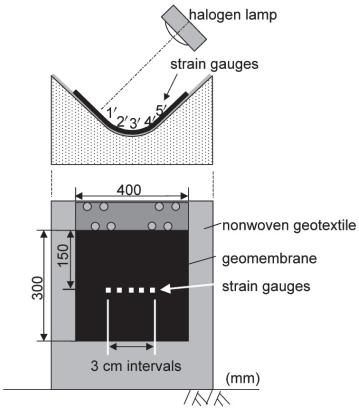

Figure 3. Experimental equipment for measuring thermal strain of geomembrane on a concave corner.

simple slope, a convex corner and a concave corner respectively. The frame of the construction was made of wood and covered with nonwoven geotextle. The geomembrane sheet was then fixed to the nonwoven textile covering and irradiated with a halogen lamp to heat it. Strain gauges were affixed on the back surface of the geomembrane sheet to measure the thermal strain. The direction of the halogen lamp and the position of strain gauges on the sheets are shown in Figures 1–3. In the simulation of a simple slope in a landfill (Figure 1), the strain gauges were fixed at the centre of the sheet, and the sheet was irradiated from a position perpendicular to the sheet. To simulate the convex corner, the strain gauges were fixed at the positions 1–5 in Figure 2, and the irradiation source was from a position perpendicular to one plane of the bent sheet. In the case of the concave corner, the strain gauges were fixed at the positions of 1′–5′ in Figure 3. In each experiment, the distance between halogen lamp and the sheet was 30 cm and the lamp was turned on until the sheet temperature was increased to 40 °C then turned off. The surface temperature of the sheet was measured using a thermal infrared imaging device and the thermal strain was measured when the sheet's temperature dropped from 40 °C to 20 °C.

2.2 *Materials*

High density polyethylene (HDPE) sheets were used in this study. Table 1 and Table 2 show the basic characteristics of the materials and the size of the sheet samples used respectively.

Table 1. Basic characteristics of the geomembrane.

Geomembrane	Elastic modulus (MPa)	Poisson ratio	Linear thermal expansion coefficient (/°C)
HDPE	500	0.458	0.00015

Table 2. Size of the geomembrane samples.

Experiments	Length (cm)	Width (cm)
Simple slope	15	20
Convex corner	30	40
Concave corner	30	40

2.3 *Estimate of thermal strain on the geomembrane using FEM calculation*

The estimate of thermal strain on the geomembrane sheet, was calculated using the finite element analysis software ANSYS. In this method, thermal strain caused by temperature change was converted into contact force for every element and the displacement of each contact was calculated from this. The relationship between heat distortion ε and temperature change Δt is defined in equation (1).

$$\varepsilon = \alpha \cdot \Delta t \tag{1}$$

where α is the linear coefficient of thermal expansion. The relationship between contact force f_m and heat distortion ε is defined in equation (2).

$$f_m = \int [B][D]\{\varepsilon\} dV \tag{2}$$

where $[B]$ is the matrix which depends on the shape of the element, $[D]$ is the matrix which depends on the property of the material. The boundary condition at the upper end is fixed, and that of lower end is free. The temperature distribution of the sheet obtained from the thermal infrared imaging device was applied to each element as thermal loading. However the friction between the sheet and the frame is not considered in this study.

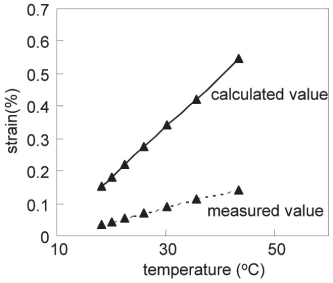

Figure 4. Measured and calculated thermal strain vs. temperature of the geomembrane on a simple slope.

2.4 RESULTS AND DISCUSSIONS

2.4.1 *Result from experiment of simple slope*

Figure 4 shows measured and calculated thermal strain vs. temperature of the geomembrane sheet. The calculated value was bigger than the measured value by about 3 times. There are several possible reasons for this. Firstly; in the experiments the strain gauge was fixed to the back surface of the sheet to avoid the situation where the temperature of the strain gauge becomes too high and exceeds the recommended temperature range. However, since the surface temperature read by the thermal image device was used in the FEM calculation, there was a temperature difference between sheet's front and back surfaces. Therefore, the strain of the back surface seemed to be smaller than that of the front surface. Secondly, it is possible the higher calculated value was because the friction between sheet and frame was not considered.

Although there was a difference between measured and calculated strain of the sheet the corresponding relationship between the strain and the temperature was rectilinear on both measured and calculated values at the range of the temperatures in this experiment.

2.4.2 *Result from experiment of convex corner*

Figure 5 shows the surface temperature distribution of the bent geomembrane sheet from the experiment using the convex corner. Since the sheet was irradiated from the right side as shown in Figure 2, only the right side of the sheet heated up. Figure 6 shows measured thermal

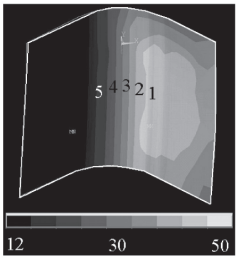

Figure 5. Thermal image of a geomembrane on a convex corner.

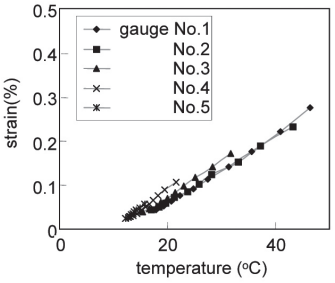

Figure 6. Measured thermal strain vs. temperature of the geomembrane on a convex corner.

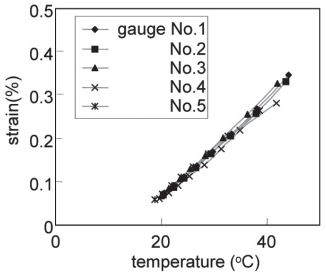

Figure 7. Calculated thermal strain vs. Temperature of the geomembrane on a convex corner.

strain vs. temperature of the geomembrane sheet, and Figure 7 shows calculated thermal strain vs. temperature. Looking at the measured values in Figure 6 the gradient of the trend line from the strain gauge at the low-temperature area (gauge No. 5) is steeper than that of the gauge on the high-temperature area (gauge No. 1). A similar variation occurs at the gauges in the middle-temperature areas. This demonstrates that the relationship between strain and temperature as shown by the gradient varies at different locations on the sheet. In contrast, the calculated values in Figure 7 show little difference in the gradient between each trend line. This is anomaly originates from the calculation method of thermal strain. Although the thermal strain on each integration point is calculated according to the temperature change of the elements at the integration point, the strain caused by the difference in the thermal strain between neighbouring elements is not considered in the FEM calculation in this study.

2.4.3 *Result from experiment of concave corner*

Figure 8 shows the surface temperature distribution of the geomembrane sheet that was taken from the experiment involving the concave corner. Compared to the temperature distribution of the convex corner (Figure 5), the difference of the sheet temperature is smaller on the concave corner. As with the experiment on the convex corner, only one plane of the bent geomembrane sheet was irradiated with the halogen lamp. However, in the concave situation unexposed planes of the sheet were also irradiated by part of the

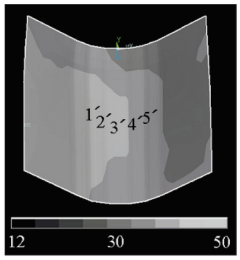

Figure 8. Thermal image of a geomembrane on a concave corner.

reflected light from another plane and so the whole sheet heated up. Figure 9 shows measured thermal strain vs. temperature of the geomembrane sheet and Figure 10 shows calculated thermal strain vs. temperature. In the experiment of the convex corner, the relationship between strain and temperature was consistent, and there was little difference based on the position of the strain gauges.

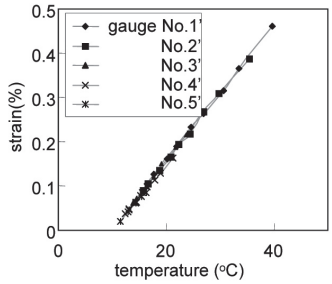

Figure 9. Measured thermal strain vs. Temperature of the geomembrane on a concave corner.

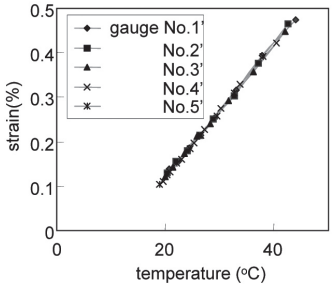

Figure 10. Calculated thermal strain vs. Temperature of the geomembrane on a concave corner.

3 ESTIMATE OF THERMAL STRESS CAUSED BY DAILY VARIATION OF SHEET TEMPERATURE IN A LANDFILL

A model calculation of a square landfill site was carried out to estimate variation of thermal stress on a geomembrane sheet during the day. The boundary conditions were set as fixed as the upper end of the slope was fixed with an anchor trench and lower end was restricted by the landfill waste. The temperature of the sheet was calculated as direct solar radiation and given as the height of the sun, azimuth angle, direction and gradient of slopes. The geomembrane sheet on every slope was assumed to be built at 12 p.m, and the thermal stress was calculated on the basis of temperature difference between readings at 6 a.m., 9 a.m. and 3 p.m. and 12 p.m. Figure 11 shows the results of the calculations. The temperature difference was largest at 6 a.m. and a reaction force of about 11 MPa was applied to the fixed ends of the north slope of the landfill. It was also found that there was more thermal stress generated in the concave corners.

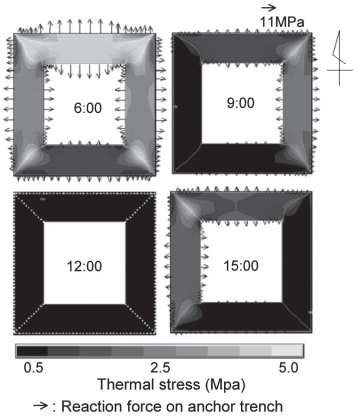

Figure 11. Thermal stress of geomembrane on a square landfill.

4 CONCLUSION

This study investigated a new method for estimating thermal stress on geomembrane sheets using temperature distribution measured by a thermal imaging device and using FEM calculations. Relationships between temperature and strain on the sheet were measured and calculated during experiments based on models of a simple slope, convex corner and concave corner.

REFERENCES

Masayuki, T., Hideki, T., Tetsuya, N. and Shigeyuki, I. (1998). "Evaluation of Thermal Stress of the Geomembren at Landfills", Proceedings of the Japan Society of Civil Engineers, No. 603, III-444, pp. 147-155.

Nozomu, K., Keisuke, K., Kazuhiro, T. and Shintaro, B. (2004). "Induced Strains in a Geosynthetics Liner Sheet Installed in a Controlled Coastal Disposal Site", Geosynthetics Engineering Journal, Vol. 19, pp. 81-86.